

Distributed quantum-information processing with fullerene-caged electron spins in distant nanotubes

Y. M. Hu,^{1,2} W. L. Yang,^{1,2} M. Feng,^{1,*} and J. F. Du^{3,†}

¹*State Key Laboratory of Magnetic Resonance and Atomic and Molecular Physics, Wuhan Institute of Physics and Mathematics, Chinese Academy of Sciences, Wuhan 430071, China*

²*Graduate School of the Chinese Academy of Sciences, Beijing 100049, China*

³*Hefei National Laboratory for Physics Sciences at Microscale and Department of Modern Physics, University of Science and Technology of China, Hefei 230026, China*

(Received 29 April 2009; published 18 August 2009)

We propose a potentially practical scheme for quantum-information processing (QIP) with spatially distributed fullerene-caged electron spins using optical and microwave manipulations. Each doped fullerene located in a semiconducting single-walled carbon nanotube is embedded in a two-mode optical cavity. The caged spins have long decoherence time and the optical manipulation makes sure short operational time. Compared to the conventional QIP proposals involving an array of fullerene-caged electron spins based on nearest-neighbor coupling, our scheme corresponds to a network which could much reduce overhead in implementing distant qubits. We discuss the experimental feasibility and challenge based on currently available techniques and we show the possibility of high-fidelity operations.

DOI: [10.1103/PhysRevA.80.022322](https://doi.org/10.1103/PhysRevA.80.022322)

PACS number(s): 03.67.Lx, 03.65.Ud, 78.67.Ch, 42.50.—p

I. INTRODUCTION

Both endohedral fullerenes [1–5] and semiconducting quantum dots (SQDs) [6] are promising candidates for future quantum-information processing (QIP). Both of them have engineerable properties and the potential for scalability and have demonstrated most of the elementary building blocks for QIP. However, SQDs suffer the strong decoherence from ambient nuclear-spin bath [7] and the fullerene-caged electron spins [1], although robust to decoherence, can be only operated by electron-spin-resonance (ESR) pulses instead of the more efficient optical pulses. Moreover, in most of the previous proposals, both the candidates for QIP are based on the nearest-neighbor spin-spin coupling, which involves a lot of overhead in conditional gating on two distant qubits and does not favor the fast implementation in large-scale QIP.

In the present work, we will explore the possibility to combine the two candidates in order to achieve a large-scale QIP with long coherent operational time and fast manipulation in optical fashion. To this end, we will consider that each doped fullerene is put into a single-walled carbon nanotube (SWCNT), called fullerene peapod [8–11]. It has been discussed recently about the charged SWCNT-SQD with a diameter 1.2 nm involving an electron initially staying in the conduction band [12,13]. Although somewhat different from the usually mentioned (In)GaAs or (Al)GaAs SQDs (called GaAs SQDs below for brevity), the SWCNT-SQD has a lot of similarities to the GaAs SQDs in optical transitions and in band configuration [14,15]. As a result, there are also some similarities in optical operations between the two kinds of SQDs.

Our key idea is to employ excitons to entangle the conduction-band electrons with the photons emitted. As long

as the conduction-band electrons have already entangled with the fullerene-caged electrons, respectively, the emitted photons would be also entangled with the caged electrons. As a result, if we entangle and then detect the two emitted photons, the state collapse would yield a mapping of the entanglement from the photons to the two distant fullerene-caged electrons.

Based on the entanglement generated, we may build a distributed QIP architecture with the peapod-fullerene-caged (simply called “caged” from now on) qubits. For convenience of our description, we call the caged electron spin the static qubit, denote the auxiliary qubit by the electron spin in the conduction band of the SWCNT-SQD, and employ the photonic polarization as the flying qubit. Some favorable features of our scheme should be mentioned. The first is the essential manipulation in optical fashion, which could much improve the operational speed and accuracy with respect to the all-ESR manipulation in previous schemes. Although it is still necessary using ESR pulses to entangle each static qubit with the corresponding auxiliary qubit, we could accomplish this entanglement simultaneously at the beginning of our scheme. Then the subsequent operations are optical performance on individual peapods. Second, the auxiliary qubits make the readout of the qubits available. In usual schemes for fullerene-based QIP, readout is one of the principal challenges in experimental implementation although there have been some wonderful ideas proposed [16]. In contrast, the auxiliary qubits in our scheme could be regarded as working readout assistants. After the implementation of a QIP task, the static qubits would be in product states ready for detection. If we prepare the auxiliary qubits in down-polarized states and perform controlled-NOT (CNOT) gates on each peapods using the static qubit as the control and the auxiliary qubit as the target, we could know the polarization of each static qubit by optically detecting the polarization of each auxiliary qubit [17].

In what follows, we will first model the procedure with emitted photons to entangle two caged spins based on virtu-

*mangfeng@wipm.ac.cn

†djf@ustc.edu.cn

ally excited excitons. Then we will discuss about the experimental feasibility and challenge regarding our scheme. We argue the potential of our scheme favorable for constructing a future solid-state quantum network [18,19]. The last section gives a short summary.

II. MODEL

We concentrate on two distant $^{15}\text{N}@C_{60}@\text{SWCNT-SQDs}$ encapsulating the static qubits A' and B' , respectively, with two auxiliary electrons A and B initially prepared, respectively, in the conduction bands of the SWCNT-SQDs. The preparation of the electrons A and B could be achieved by turnstile injectors [20–22]. As shown in Fig. 1, to avoid low collection rate of the emitted photons due to spontaneous emission and finite-angle coverage of the collector, we consider the two peapods to be embedded, respectively, in separate two-mode optical cavities, which could absorb the emitted photons in resonance in a Raman process and leak them away along a fixed direction. The cavities could be micropillar cavities formed in substrates [23] or in photonic crystals [24] and should be identical with two orthogonally polarized modes in each. Specifically, we encode the static qubits in the electron-spin levels $|\pm 3/2\rangle$ of the doped atom ^{15}N and the auxiliary qubit in the electron-spin level $|\pm 1/2\rangle$ in the conduction band of the SWCNT-SQD. For clarity of following description, we label $|-1/2\rangle = |\downarrow\rangle_k$, $|1/2\rangle = |\uparrow\rangle_k$, $|-3/2\rangle = |\downarrow\rangle_{k'}$, and $|3/2\rangle = |\uparrow\rangle_{k'}$ with $k=A, B$ and $k'=A', B'$.

A. Entanglement of the static and auxiliary qubits

The first step of our proposal is to entangle the static and the auxiliary qubits. Under the magnetic field gradient $B_0(x)$, the static and the auxiliary qubits could be coupled by dipolar interaction with the Ising type [25]. Since this magnetic dipolar coupling strength is about 50 MHz in the case of the spin-spin distance 1.14 nm [1,2], we may achieve CNOT operations by selective ESR pulses. In our case, we may suppose that the two qubits are distant by about 0.8 nm including the radius of the fullerene cage and the thickness of the SWCNT. So the spin-spin coupling should be larger than 50 MHz. As a result, once the auxiliary qubit is prepared in a superposition state, CNOT operations would yield the entanglement between the static and the auxiliary qubits [25]

$$(|\uparrow\uparrow\rangle + |\downarrow\downarrow\rangle)_{AA'}(|\uparrow\uparrow\rangle + |\downarrow\downarrow\rangle)_{BB'}/2.$$

B. Entanglement of distant qubits

For our purpose to entangle the distant static qubits by leaking photons, we have to produce excitons. As excitons are usually with the lifetime of the order of picoseconds, if we have a resonant excitation, the exciton would quickly decay with a photon spontaneously emitted. Specifically, with linearly polarized laser pulses employed, if the electron A or B in the conduction band is initially up (down) polarized, due to the Pauli exclusion principle under a polarized radiation, only the excitonic state $|1/2\rangle_{con-e}|-1/2\rangle_{con-e}|1/2\rangle_{val-h}|-1/2\rangle_{con-e}|1/2\rangle_{con-e}|-1/2\rangle_{val-h}$ could be produced, where the subscripts denote the conduction-band

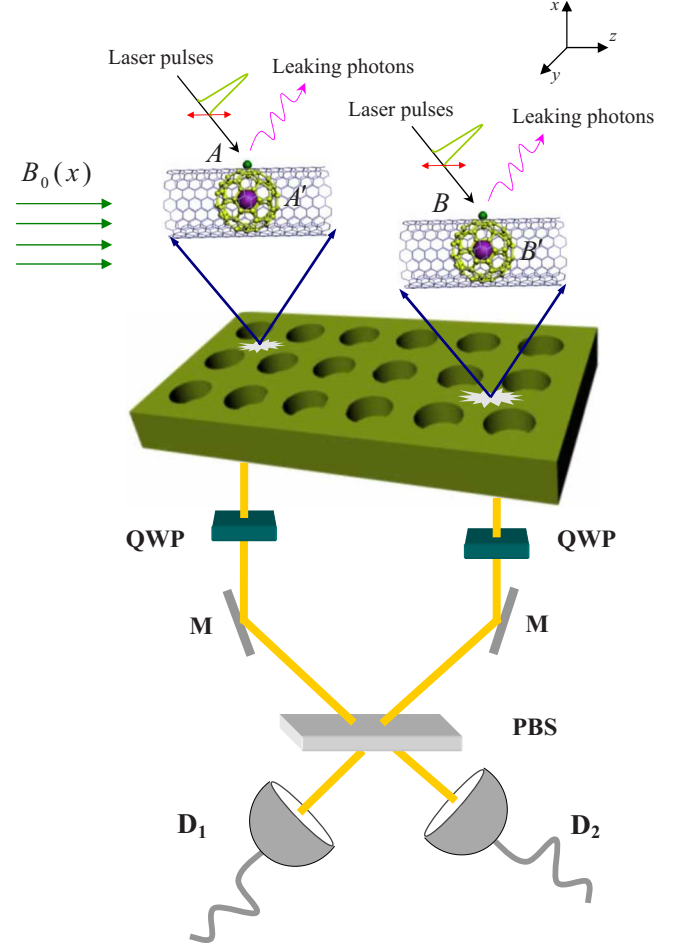


FIG. 1. (Color online) Schematic setup for generation of the entanglement between two caged electron spins in two distant peapods, where each fullerene is located in a SWCNT-SQD embedded in a two-mode optical cavity. We show here the cavity in photonic crystal as an example. Actually, the cavity required could also be a micropillar cavity in a substrate. The static qubits A' and B' are caged in the peapods and the auxiliary qubits A and B are bound in the conduction bands of the SWCNT-SQDs. The magnetic field gradient $B_0(x) = \frac{\partial B_0}{\partial x} \delta x \hat{e}_z$ applied along the nanotube axis is used to entangle the static and auxiliary qubits and to define the quantization axis. The lasers with linear polarization are radiated to generate single σ_{\pm} polarized photons by STIRAP. The quarter-wave plates (QWPs) transform left- and right-polarized photons to be horizontally and vertically polarized, respectively. PBS is the polarized beam splitter which transmits $|H\rangle$ and reflects $|V\rangle$. M is the mirror and D_i , with $i=1, 2$, are the single-photon detectors.

electron (*con-e*) and the valence-band hole (*val-h*) [26]. In our scheme, we consider the consequence of spin-orbit interaction in the SWCNT-SQD [27], which yields different excitation energies of the excitons. For clarity, we will label with $|U\rangle(|D\rangle)$ the excitonic states regarding positive (negative) orbital magnetic moment originated from different valleys in the SWCNT-SQD [13,27]. We require the excitonic state $|U\rangle(|D\rangle)$ decaying back to $|-1/2\rangle_{con-e}(|1/2\rangle_{con-e})$ with a $\sigma_{+}(\sigma_{-})$ polarized photon emitted. This could be achieved by a stimulated Raman adiabatic passage (STIRAP) [28] along with a $\sigma_{+}(\sigma_{-})$ polarized cavity mode. To avoid spontaneous

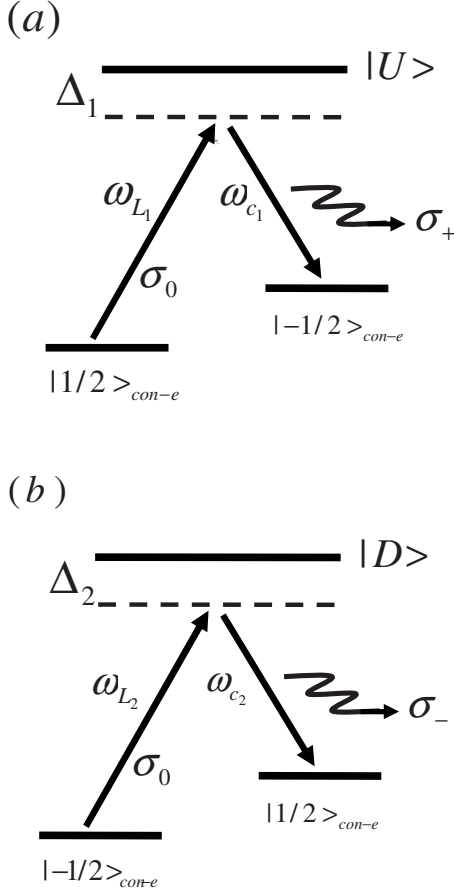


FIG. 2. Generation of single photons via virtually exciting excitons, where (a) describes the process from the initial state $|1/2\rangle_{con-e}$ via the virtual exciton $|U\rangle$ and (b) is for the process from the initial state $|-1/2\rangle_{con-e}$ via the virtual exciton $|D\rangle$. ω_{L_i} and ω_{c_i} ($i=1,2$) are, respectively, frequencies of the laser and the cavity mode and Δ_i is the corresponding detuning. $\sigma_{j=0,+,-}$ denote linearly, right-, and left-polarized photons, respectively.

emission of the exciton, large detuning is necessary, as shown in Fig. 2. In this context, we have only virtually excited the excitons in this process and consequently the main detrimental factor in our treatment is the cavity decay, instead of the excitonic decay. Considering two microcavities and two linearly polarized lasers radiated with ω_{L_1} and ω_{L_2} , respectively, we may rewrite the process as

$$\begin{aligned}
 & (|\uparrow\uparrow\rangle + |\downarrow\downarrow\rangle)_{AA'}(|\uparrow\uparrow\rangle + |\downarrow\downarrow\rangle)_{BB'}|00\rangle_{I,II}/2 \rightarrow (|\downarrow\uparrow\rangle_{AA'}|\sigma_+\rangle_I \\
 & + |\uparrow\downarrow\rangle_{AA'}|\sigma_-\rangle_I)(|\downarrow\uparrow\rangle_{BB'}|\sigma_+\rangle_{II} + |\uparrow\downarrow\rangle_{BB'}|\sigma_-\rangle_{II})/2 \\
 & \rightarrow (|\downarrow\uparrow\rangle_{AA'}|\downarrow\uparrow\rangle_{BB'} + |\uparrow\downarrow\rangle_{AA'}|\uparrow\downarrow\rangle_{BB'})|00\rangle_{I,II}/\sqrt{2}, \quad (1)
 \end{aligned}$$

where, for simplicity, we have denoted the vacuum states of the two microcavities by $|00\rangle_{I,II}$, with $|i\rangle_j$ the mode of the j th microcavity, $i=\sigma_+$ or σ_- , and $j=I$ or II . The second step of the equation is accomplished by STIRAP associated with the virtually excited $|U\rangle$ and $|D\rangle$. The last step is the yield from the simultaneous clicks at the two detectors D_1 and D_2 : the entanglement of A , A' , B , and B' .

To single out the entanglement between A' and B' , we perform optical pulses on the electrons A and B for Hadamard transformation $H=(\sigma_x+\sigma_z)/\sqrt{2}$, i.e., $|\uparrow\rangle_{A(B)} \rightarrow (1/\sqrt{2})(|\uparrow\rangle+|\downarrow\rangle)_{A(B)}$ and $|\downarrow\rangle_{A(B)} \rightarrow (1/\sqrt{2})(|\uparrow\rangle-|\downarrow\rangle)_{A(B)}$ and then we carry out the STIRAP again. But this time, we only employ the laser pulse with frequency ω_{L_1} to virtually excite the excitons $|U\rangle$ in the two peapods. As a result, the down-polarized spin states $|-1/2\rangle_{con-e}$ would remain unchanged and the simultaneous detection of the leaking photons out of the two microcavities leads to the system collapsing to the entangled state $(|\uparrow\rangle_{A'}|\uparrow\rangle_{B'}+|\downarrow\rangle_{A'}|\downarrow\rangle_{B'})/\sqrt{2}$, based on which, if necessary, other three Bell states are also available simply by ESR pulses on one of the static qubits. Therefore, Bell states could be fully generated in our scheme.

C. Treatment involving dissipation

Equation (1) and the relevant consideration in above subsection are for a simple demonstration of the process for entangling two distant qubits. In order to have a more strict treatment for above implementation, we have to make some assumptions and simplification, with which we could present an analytical treatment and assess the implementation time and the efficiency of our scheme.

Due to the virtual excitation of the excitons, we may assume the spontaneous emission from the exciton to be negligible in above STIRAP. This assumption could be justified using a recent measurement of a long excitonic decay time (i.e., 8.7 ns) in the case of large detuning in a GaAs quantum dot (QD) system [24]. As long as our implementation time is comparable to picoseconds, we may reasonably omit the effect of the excitonic decay in our treatment. As a result, the main detrimental factor is the cavity decay, which is of the order of picoseconds [24]. To improve the success rate of our scheme, however, we will assume to work with the microcavities with higher Q factors than in [24], which ensures the decay rate to be smaller than other characteristic frequencies. Considering the weak cavity dissipation, we have the effective Hamiltonian for above STIRAP in units of $\hbar=1$ as

$$\begin{aligned}
 H_{eff} = \sum_{m=1}^2 \left[\frac{V_m}{2} (|\downarrow\rangle_m \langle \uparrow| a_m^\dagger + |\uparrow\rangle_m \langle \downarrow| b_m^\dagger + \text{H.c.}) \right. \\
 \left. - i\kappa_m (a_m^\dagger a_m + b_m^\dagger b_m) \right], \quad (2)
 \end{aligned}$$

where a_m^\dagger (a_m) and b_m^\dagger (b_m) are, respectively, the creation (annihilation) operators for the cavity modes with $m=1,2$ and $V_m=\Omega_m g_m/2\Delta_m$ denotes the effective Rabi frequency with Ω_m and g_m the couplings due to the laser and the cavity mode, respectively. For simplicity, we may assume in following treatment $V_1=V_2=V$, which could be achieved by appropriately adjusting the experimental parameters and we also assume $\kappa_1=\kappa_2=\kappa$. Under the condition $\kappa \ll V$, we might try to solve the time evolution of the system analytically using quantum trajectory approach [29].

Starting from the initially entangled state $(|\uparrow\uparrow\rangle + |\downarrow\downarrow\rangle)_{AA'}(|\uparrow\uparrow\rangle + |\downarrow\downarrow\rangle)_{BB'}|00\rangle_{I,II}/2$, we may directly obtain the time evolution of the system at any time (see the Appendix for details), from which we could single out some desired spin-entangled states by coincident measurement on the leak-

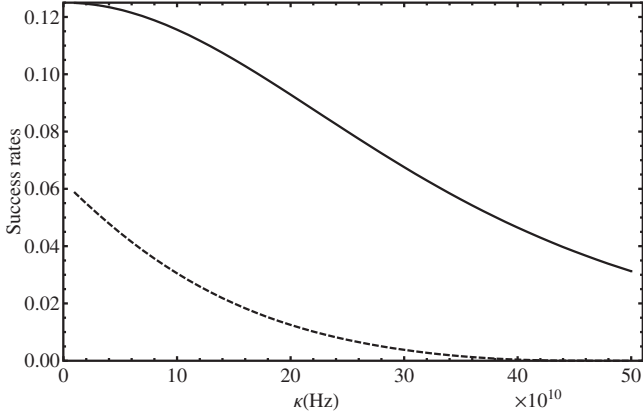


FIG. 3. Success probabilities P_1 and P_2 with respect to the cavity decay rate κ , where we set $\Omega_1=10$ meV ≈ 15.2 THz, $g_1=1$ meV ≈ 1.52 THz, and $\Delta_1=15$ meV ≈ 22.8 THz. P_1 and P_2 , defined in the text, are plotted by solid and dashed curves. Strictly considering the condition $V \gg \kappa$, we only need to show $\kappa < 500$ GHz. The calculation applied to the exciton $|D\rangle$ is similar.

ing photons out of the microcavities. For example, by directing the two leaking photons to a polarization beam splitter (PBS), we may obtain the output state $(|\downarrow\uparrow\rangle_{AA'}|\downarrow\uparrow\rangle_{BB'} + |\uparrow\downarrow\rangle_{AA'}|\uparrow\downarrow\rangle_{BB'})/\sqrt{2}$ by coincident detection with the success rate

$$P_1 = |c_2|^4/[8(c_1^2 + |c_2|^2)^2],$$

where c_1 and c_2 are defined in the Appendix.

With further effort, namely, the virtual excitation of the excitonic states $|U\rangle$ again, we could obtain the entangled state $|\Psi\rangle_{\text{Bell}} = (|\uparrow\rangle_{A'}|\uparrow\rangle_{B'} + |\downarrow\rangle_{A'}|\downarrow\rangle_{B'})/\sqrt{2}$ with the success rate

$$P_2 = |c_2|^4/[4(c_1^2 + |c_2|^2 + 1)^2].$$

Both P_1 and P_2 are simulated in Fig. 3 with respect to the decay rate. The success rates are much lower than our expectation because we obtain the entangled states from 16 terms of the evolved state and also from the PBS with intrinsic 50% success rate. Nevertheless, we argue that our scheme could be accomplished within 30 ns due to the fast optical operations employed. Considering the effective Rabi frequency $V=0.5$ THz and the cavity decay rate $\kappa=15$ GHz, we have the implementation time for entangling two static qubits: $T \approx 2(\pi/V+1/\kappa)=150$ ps, where 2 means twice the excitations of the excitons. This also implies that an actual accomplishment of the entanglement of two static qubits, including the success rates $P_1=0.125$ and $P_2=0.05$, takes 26 ns.

III. DISCUSSION

A. Feasibility and challenge

The single electron was proposed to be injected into the conduction band of the semiconducting SWCNT by turnstile injectors [20–22]. Recent experiments have shown single-electron effect in the conduction band of the SWCNT [11,30]. On the other hand, due to the similarity in optical

and band structural characteristics between GaAs SQD and SWCNT-SQD, we may assume the similarity also existing in operational scheme and skill between the two systems. As it has been achieved in charged GaAs SQDs with the optically driven excitons and fast manipulation of single-electron spins in the conduction band [31], we could hope to accomplish similar operations with the SWCNT-SQD [13] soon. For example, recent experimental effort has achieved optical generation of excitons in SWCNT-SQD, probably around charged defects [14,15].

As discussed in Sec. II C, the entanglement of two distant qubits is accomplished within 30 ns. In fact, if including the entanglement between the caged electron spin and the conduction-band electron spin, this time would be of the order of microseconds. In contrast, in conventional ideas to entangle two distant caged electron spins by nearest-neighbor coupling [1–5], we have to carry out many swap operations with each swap consisting of three CNOT gates. As each CNOT gating takes a time T on the order of microseconds, we have to spend $3nT$ for accomplishing n swap operations. In this sense, our proposal, although intrinsically probabilistic and involving different subsystems and degrees of freedom, entangles two distant caged qubits much more efficiently than in [1–5].

For the measurement of the auxiliary qubits, which is related to the readout of the qubits in our scheme, we have also checked the experimental progress in GaAs SQDs. While the usual idea with spin-to-charge conversion would destroy the electron in the conduction band [32], the recently achieved experiment for nondestructive optical detection using Kerr rotation or Faraday rotation for GaAs SQD would probably be applicable to our case [33]. An alternative between [32,33] is to radiate the SWCNT-SQD by a laser, e.g., with frequency ω_{L_1} [17]. If the auxiliary qubit is in $|\uparrow\rangle_k$ ($k=A,B$), a σ_+ photon would be produced and finally leaked out of the cavity. As a result, the detection of the leaking photon corresponds to the auxiliary qubit state in $|\uparrow\rangle_k$ ($k=A,B$). The cavity helps collect the produced photon, which could much enhance the detection efficiency.

Ohmic coupling of the excitons to one-dimensional acoustic phonons in SWCNTs has been intensively studied recently. Although it does not change the efficiency of the spin pumping, the coupling would yield dephasing of the excitons, which handicaps the implementation of our scheme. Normally, the exciton-phonon coupling strongly relies on the size of the SQD and the recent studies [14] have shown that this kind of coupling appears mainly in very-small-sized SWCNT-SQDs (≈ 10 nm). So if we consider the SWCNT-SQD with the length longer than 20 nm [13,15], the detrimental effect from one-dimensional acoustic phonons would be much suppressed in our case. In addition, dynamical decoupling techniques [34], also called bang-bang control, could effectively suppress the dephasing due to coupling to the acoustic phonon in GaAs SQDs. Recent study has shown the possibility with dynamical decoupling technique to extend hopefully the coherent time of excitons by at least 2 orders of magnitude [35]. As a result, if we apply the bang-bang control to our case, the excitonic coherence time would be expected to be longer than 3 ns, which guarantees a safe implementation of our scheme.

On the other hand, we have considered putting the single SWCNT-SQDs respectively into microcavities, which could effectively enhance the coupling and the implementation efficiency and could also reduce the decay rate of the excitons. We have noticed the achievement of the GaAs SQDs tightly confined in micropillar cavities or defects in photonic crystal. The similar confinement would be available soon for the SWCNT-SQDs [13].

Moreover, as we employed STIRAP to avoid spontaneous emission from the exciton, the effective Rabi frequency V in STIRAP, smaller than either Ω_m or g_m due to the condition $\Omega_m, g_m \ll \Delta_m$, makes our implementation slower than a resonant excitation of the exciton. In this context, to have an efficient entanglement of the static qubits in our scheme, we need stronger couplings. But the currently reachable coupling between the cavity mode and the GaAs SQD is not strong enough for carrying out our scheme. As shown in Fig. 3, the values we used in our calculation are larger than currently available values regarding GaAs SQDs by 3 degrees of magnitude.

B. Estimate of the efficiency of our implementation

Both decoherence and imperfection would yield errors in the implementation. In our case, besides the cavity decay considered above, decoherence regarding the conduction-band electron spin and the virtually excited exciton, although occurring on the order of nanoseconds, would also probably affect our implementation. However, since we could accomplish our operations on excitons within 150 ps, the detrimental effect of the decoherence on the efficiency of our implementation would be very limited. On the other hand, the main imperfect factors include (1) the operational offset regarding the qubits and the auxiliary qubits and (2) the photon loss due to cavity absorption and scattering, the fiber absorption, and the detector inefficiency. As our optical implementation is very fast and there is possibility of structural inhomogeneity in the peapod, we have to pay attention to the inaccuracy in operations. Evidently, the operational imperfection would mainly lead to infidelity. In contrast, the photon loss does not affect the fidelity, but only the efficiency in our scheme.

We may simply assess the efficiency of our scheme below. The failure rate associated with the decays of the conduction-band electron spin and the exciton could be assumed to be about 1% [$\approx (\Omega_m/2\Delta_m)^2$] and the dark count rate of current single-photon detector is 100 Hz, yielding the failure rate 10^{-9} in our case. Considering other failure rates regarding fiber absorption and cavity scattering and absorption to be about 6%, we have the success rate $(1-1\%)^6(1-10^{-9})^4(1-6\%)P_1P_2=0.88P_1P_2$, where the sixth power is due to the six excitons virtually generated, the fourth power is related to four detections of the leaking photons, and P_1 and P_2 are, respectively, the intrinsic success rates of our scheme shown in Fig. 3.

C. Quantum communication and computation

Our scheme could be straightforwardly extended to multipartite entangled states. Figure 4 presents an example for

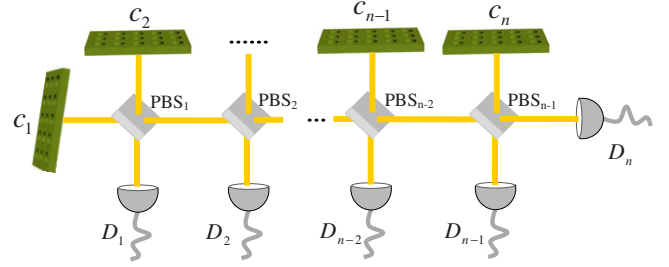


FIG. 4. (Color online) Schematic setup for achieving an n -qubit GHZ state of the caged electron spins, where c_k with $k = 1, 2, \dots, n$ includes the k th peapod embedded in a photonic crystal cavity and also includes a QWP. D_k is the single-photon detector. When all the detectors click, we achieve the GHZ state. Since each photon going through a PBS splits into two parts associated with different polarizations, for meeting the requirement for coincident detection, we must make sure appropriate path lengths for different polarization components of each photon.

generation of an n -qubit Greenberger-Horne-Zeilinger (GHZ) state $(|\downarrow\rangle_1|\downarrow\rangle_2\cdots|\downarrow\rangle_n+|\uparrow\rangle_1|\uparrow\rangle_2\cdots|\uparrow\rangle_n)/\sqrt{2}$ of the spatially separate caged spins by simultaneous clicks of the detectors. This implies the construction of a quantum network of peapod-based qubits, in which QIP tasks, such as teleportation [36], state transfer, and universal quantum gating [37] could be accomplished.

Actually, with slight modification, we could also generate other frequently mentioned entangled states, such as the cluster states [38]. As single-qubit operations and measurement are available for the auxiliary qubit and the swap operation would exchange the states between the qubit and the auxiliary qubit, one-way quantum computing [39] with caged qubits could be carried out in our SWCNT-SQD system. This implies that no rewiring of the hard wares mentioned above is necessary for accomplishing a meaningful QIP task.

In the context of a quantum network, each photonic crystal or each peapod plays as a quantum node and the generated entanglement between the nodes works as quantum channel. In our case, there are different degrees of freedom in each quantum node to store and process quantum information. The flying photons help to set up quantum channels. We had noticed considerable experimental efforts to achieve quantum network using atomic qubits [19]. In contrast, our present scheme, with the possibility of entangling and operating caged electron spins in high fidelity, paves a promising way toward the quantum network using solid-state qubits.

IV. CONCLUSION

In summary, we have proposed a potentially practical scheme for QIP with electron spins caged in distant peapods. Compared to previous works for entangling fullerene-caged electron spins using nearest-neighbor coupling [1–5], our scheme could generate entanglement among distant caged qubits with much less overhead. This makes it possible to efficiently produce some entangled states with the spatially separate peapods.

Our proposal consists of different subsystems, such as doped fullerenes, SWCNTs, microcavities, and linear optical

elements. Each of these subsystems had been employed in QIP schemes previously. We have shown in this paper the composition of them could achieve a quantum network with quantum information transferred and processed in and between the qubits distributed at spatially different locations. Although ESR operations are still necessary in some steps, the generation of entanglement in our proposal mainly relies on the fast manipulation of optics, such as the production of excitons, photonic leakage, transmission, and detection. Our scheme is intrinsically probabilistic, but it could much reduce the overhead with respect to conventional fullerene-qubit schemes with nearest-neighbor coupling and could reach high fidelity in a repeat-until-success fashion. Although some of the operations in our scheme are still unreachable with current techniques, we argue that our scheme would be helpful for achieving large-scale QIP setup with fullerene-based qubits in the near future.

Further discussion would involve nuclear spins of the doped atoms. As ^{15}N has the nuclear spin $I=1/2$ which is of much longer coherence time than the corresponding electron spin, it is better to encode qubits in nuclear spins of the doped atoms but employ corresponding electron spins as ancilla [3,5].

ACKNOWLEDGMENTS

Y.M.H. is grateful to Zhenyu Xu and Yong Yang for their help. This work is mainly supported by NNSF of China under Contract No. 10774163. J.F.D. acknowledges thankfully support from Chinese Academy of Sciences, NNSF of China, and the National Fundamental Research Program of China.

APPENDIX

Under the condition $\kappa \ll V$, we may employ quantum trajectory approach [29] to solve the time evolution of Eq. (2) analytically. Starting from the initially entangled state $\Psi(0) = (|\uparrow\uparrow\rangle + |\downarrow\downarrow\rangle)_{AA'}(|\uparrow\uparrow\rangle + |\downarrow\downarrow\rangle)_{BB'}|00\rangle_{II}/2$, direct deduction leads to

$$\begin{aligned} \Psi(t) = & c_1^2 |\downarrow\downarrow\downarrow\downarrow\rangle_{AA'BB'} |00\rangle_{II} + c_1 c_2 |\downarrow\downarrow\downarrow\downarrow\rangle_{AA'BB'} |0\rangle_I |\sigma_-\rangle_{II} \\ & + c_2^2 |\downarrow\downarrow\uparrow\uparrow\rangle_{AA'BB'} |00\rangle_{II} + c_1 c_2 |\downarrow\downarrow\uparrow\uparrow\rangle_{AA'BB'} |0\rangle_I |\sigma_+\rangle_{II} \\ & + c_1 c_2 |\uparrow\downarrow\downarrow\downarrow\rangle_{AA'BB'} |\sigma_-\rangle_I |0\rangle_{II} \\ & + c_2^2 |\uparrow\downarrow\downarrow\downarrow\rangle_{AA'BB'} |\sigma_-\rangle_I |\sigma_-\rangle_{II} \\ & + c_1 c_2 |\uparrow\downarrow\uparrow\uparrow\rangle_{AA'BB'} |\sigma_-\rangle_I |0\rangle_{II} \\ & + c_2^2 |\uparrow\downarrow\uparrow\uparrow\rangle_{AA'BB'} |\sigma_-\rangle_I |\sigma_+\rangle_{II} + c_1^2 |\uparrow\uparrow\downarrow\downarrow\rangle_{AA'BB'} |00\rangle_{II} \\ & + c_1 c_2 |\uparrow\uparrow\downarrow\downarrow\rangle_{AA'BB'} |0\rangle_I |\sigma_-\rangle_{II} + c_1^2 |\uparrow\uparrow\uparrow\uparrow\rangle_{AA'BB'} |00\rangle_{II} \\ & + c_1 c_2 |\uparrow\uparrow\uparrow\uparrow\rangle_{AA'BB'} |0\rangle_I |\sigma_+\rangle_{II} \\ & + c_1 c_2 |\downarrow\uparrow\downarrow\downarrow\rangle_{AA'BB'} |\sigma_+\rangle_I |0\rangle_{II} \\ & + c_2^2 |\downarrow\uparrow\uparrow\downarrow\rangle_{AA'BB'} |\sigma_+\rangle_I |\sigma_-\rangle_{II} \\ & + c_1 c_2 |\downarrow\uparrow\uparrow\uparrow\rangle_{AA'BB'} |\sigma_+\rangle_I |0\rangle_{II} \\ & + c_2^2 |\downarrow\uparrow\downarrow\uparrow\rangle_{AA'BB'} |\sigma_+\rangle_I |\sigma_+\rangle_{II}, \end{aligned}$$

where $c_1 = e^{-\kappa t/2} [(\kappa/\eta) \sin(\eta t/2) + \cos(\eta t/2)]$, $c_2 = -i(\kappa/\eta) \times e^{-\kappa t/2} \sin(\eta t/2)$, and $\eta = \sqrt{V^2 - \kappa^2}$. We have not normalized the evolved state in above expression for simplicity, but will consider normalization later when numerically calculating the success rates P_1 and P_2 .

-
- [1] W. Harnett, Phys. Rev. A **65**, 032322 (2002).
[2] D. Suter and K. Lim, Phys. Rev. A **65**, 052309 (2002).
[3] J. Twamley, Phys. Rev. A **67**, 052318 (2003).
[4] M. Feng and J. Twamley, Phys. Rev. A **70**, 032318 (2004).
[5] C. Ju, D. Suter, and J. Du, Phys. Rev. A **75**, 012318 (2007).
[6] D. Loss and D. P. DiVincenzo, Phys. Rev. A **57**, 120 (1998); A. Imamoglu, D. D. Awschalom, G. Burkard, D. P. DiVincenzo, D. Loss, M. Sherwin, and A. Small, Phys. Rev. Lett. **83**, 4204 (1999); L. Robledo, J. Elzerman, G. Jundt, M. Atatüre, A. Hogege, S. Falt, and A. Imamoglu, Science **320**, 772 (2008).
[7] G. Burkard, D. Loss, and D. P. DiVincenzo, Phys. Rev. B **59**, 2070 (1999); I. A. Merkulov, Al. L. Efros, and M. Rosen, *ibid.* **65**, 205309 (2002).
[8] B. W. Smith, M. Monthieux, and D. E. Luzzi, Nature (London) **396**, 323 (1998).
[9] A. Rochefort and CERCA-Groupe Nanostructures Phys. Rev. B **67**, 115401 (2003); M.-H. Du and H.-P. Cheng, *ibid.* **68**, 113402 (2003); H. Chadli, A. Rahmani, K. Sbai, P. Hermet, S. Rols, and J. L. Sauvajol, *ibid.* **74**, 205412 (2006).
[10] P. Utko, J. Nygård, M. Monthieux, and L. Noé, Appl. Phys. Lett. **89**, 233118 (2006); L. Ge, B. Montanari, J. H. Jefferson, D. G. Pettifor, N. M. Harrison, and G. A. D. Briggs, Phys. Rev. B **77**, 235416 (2008).
[11] C. H. L. Quay, J. Cumings, S. J. Gamble, A. Yazdani, H. Kataura, and D. Goldhaber-Gordon, Phys. Rev. B **76**, 073404 (2007).
[12] R. B. Weisman and S. M. Bachilo, Nano Lett. **3**, 1235 (2003).
[13] C. Galland and A. Imamoglu, Phys. Rev. Lett. **101**, 157404 (2008).
[14] A. Högele, C. Galland, M. Winger, and A. Imamoglu, Phys. Rev. Lett. **100**, 217401 (2008).
[15] C. Galland, A. Högele, H. E. Türeci, and A. Imamoglu, Phys. Rev. Lett. **101**, 067402 (2008).
[16] M. Feng and J. Twamley, Phys. Rev. A **70**, 030303(R) (2004); Europhys. Lett. **69**, 699 (2005); J. Twamley, D. W. Utami, H.-S. Goan, and G. Milburn, New J. Phys. **8**, 63 (2006); M. Feng, G. J. Dong, and B. Hu, *ibid.* **8**, 252 (2006).
[17] E. Pazy, E. Biolatti, T. Calarco, I. D'Amico, P. Zanardi, F. Rossi, and P. Zoller, Europhys. Lett. **62**, 175 (2003); M. Feng, I. D'Amico, P. Zanardi, and F. Rossi, Phys. Rev. A, **67**, 014306 (2003).
[18] J. I. Cirac, P. Zoller, H. J. Kimble, and H. Mabuchi, Phys. Rev. Lett. **78**, 3221 (1997).
[19] H. J. Kimble, Nature (London) **453**, 1023 (2008).
[20] L. P. Kouwenhoven, A. T. Johnson, N. C. van der Vaart, C. J.

- P. M. Harmans, and C. T. Foxon, *Phys. Rev. Lett.* **67**, 1626 (1991). This turnstile injector was applied on a GaAs SQD, but it might be also applied to a SWCNT-SQD [21,22] due to band structural similarity between the two kinds of SQDs.
- [21] D. Gunlycke, J. H. Jefferson, T. Rejec, A. Ramšak, D. G. Pettifor, and G. A. D. Briggs, *J. Phys.: Condens. Matter* **18**, S851 (2006).
- [22] S. C. Benjamin, A. Ardavan, G. A. D. Briggs, D. A. Britz, D. Gunlycke, J. Jefferson, M. A. G. Jones, D. F. Leigh, B. W. Lovett, A. N. Khlobystov, S. A. Lyon, J. J. L. Morton, K. Porfyrakis, M. R. Sambrook, and A. M. Tyryshkin, *J. Phys.: Condens. Matter* **18**, S867 (2006).
- [23] J. P. Reithmaier, G. Sek, A. Löffler, C. Hofmann, S. Kuhn, S. Reitzenstein, L. V. Keldysh, V. D. Kulakovskii, T. L. Reinecke, and A. Forchel, *Nature (London)* **432**, 197 (2004); A. Dousse, J. Suffczyński, R. Braive, A. Miard, A. Lemaître, I. Sagnes, L. Lanco, J. Bloch, P. Voisin, and P. Senellart, *Appl. Phys. Lett.* **94**, 121102 (2009).
- [24] K. Hennessy, A. Badolato, M. Winger, D. Gerace, M. Atatüre, S. Gulde, S. Fält, E. L. Hu, and A. Imamoglu, *Nature (London)* **445**, 896 (2007) However, we have not found similar results for SWCNT-SQDs yet.
- [25] W. L. Yang, H. Wei, X. L. Zhang, and M. Feng, *Phys. Rev. A* **78**, 054301 (2008).
- [26] For simplicity, we assume the SQDs to be identical in our treatment. Moreover, we employ the light holes $|\pm 1/2\rangle_{val-h}$ to produce the excitons. Actually, our scheme is directly applicable to the heavy holes $|\pm 3/2\rangle_{val-h}$.
- [27] F. Kuemmeth, S. Ilani, D. C. Ralph, and P. L. McEuen, *Nature (London)* **452**, 448 (2008).
- [28] STIRAP has been widely employed using differently polarized photons in various physical systems for keeping coherent operations, for example, in N. V. Vitanov and S. Stenholm, *Phys. Rev. A* **55**, 648 (1997). The STIRAP has also been involved in QIP proposals and experiments for QIP with SQDs [10(a)]. Employment of multimode microcavities could much enhance the interaction of interest. See [23,24].
- [29] M. B. Plenio and P. L. Knight, *Rev. Mod. Phys.* **70**, 101 (1998).
- [30] B. Gao, D. C. Glattli, B. Placais, and A. Bachtold, *Phys. Rev. B* **74**, 085410 (2006).
- [31] D. Press, T. D. Ladd, B. Zhang, and Y. Yamamoto, *Nature (London)* **456**, 218 (2008); J. Berezovsky, M. H. Mikkelsen, N. G. Stoltz, L. A. Coldren, and D. D. Awschalom, *Science* **320**, 349 (2008); A. Gleilich, S. E. Economou, S. Spatzek, D. R. Yakovlev, D. Reuter, A. D. Wieck, T. L. Reinecke, and M. Bayer, *Nat. Phys.* **5**, 262 (2009).
- [32] J. M. Elzerman, R. Hanson, L. H. Willems van Beveren, B. Witkamp, L. M. K. Vandersypen, L. P. Kouwenhoven, *Nature (London)* **430**, 431 (2004).
- [33] J. Berezovsky, M. H. Mikkelsen, O. Gywat, N. G. Stoltz, L. A. Coldren, and D. D. Awschalom, *Science* **314**, 1916 (2006); M. Atatüre, J. Dreiser, A. Badolato, and A. Imamoglu, *Nat. Phys.* **3**, 101 (2007).
- [34] L. Viola and S. Lloyd, *Phys. Rev. A* **58**, 2733 (1998).
- [35] T. E. Hodgson, L. Viola, and I. D'Amico, *Phys. Rev. B* **78**, 165311 (2008).
- [36] C. H. Bennett, G. Brassard, C. Crépeau, R. Jozsa, A. Peres, and W. K. Wootters, *Phys. Rev. Lett.* **70**, 1895 (1993).
- [37] D. Gottesman and I. L. Chuang, *Nature (London)* **402**, 390 (1999).
- [38] H. J. Briegel and R. Raussendorf, *Phys. Rev. Lett.* **86**, 910 (2001).
- [39] R. Raussendorf and H. J. Briegel, *Phys. Rev. Lett.* **86**, 5188 (2001).